J Ind Microbiol Biotechnol (2010) 37:935–942
DOI 10.1007/s10295-010-0742-5

ORIGINAL PAPER

Electrooptical monitoring of cell polarizability and cell size in aerobic *Escherichia coli* batch cultivations

Stefan Junne · M. Nicolas Cruz-Bournazou · Alexander Angersbach · Peter Götz

Received: 29 June 2009 / Accepted: 6 May 2010 / Published online: 29 May 2010

Abstract The time-dependent development of cell polarizability and length in *Escherichia coli* batch fermentations were observed at-line with electrooptical measurements. While using a measurement system with fully automated sample preparation, the development of these properties can be observed with a comparable high frequency (six measurements per hour). The polarizability as well as the mean cell length both increase soon after inoculation and then decline from the growth phase on until the stationary phase is reached. Based on the dynamic behavior of polarizability, the growth phase can be divided into four distinct stages. Changes in the cultivation temperature or the pre-cultivation conditions lead to alterations in the development of the polarizability and mean cell length. Based on the frequency disperse of polarizability measured at four different frequencies from 210 to 2,100 kHz, a prediction model is established that is based on the relation of the polarizability to the metabolic activity. Applying multi-linear partial least squares methods (N-PLS), the model is able to predict the specific acetate synthesis and uptake with a root mean square error of prediction of 0.19 (6% of the mean). The method represents a tool for characterization of different stages with respect to microbial metabolic activity and the energy balance during batch cultivations.

Keywords Electrooptical measurement · Cell polarizability · Cell length · *Escherichia coli* · Cultivation · Acetate synthesis

P. Götz (✉)
Department of Bioprocess Engineering, Beuth University of Applied Sciences, Seestrasse 64, 13347 Berlin, Germany
e-mail: Peter.Goetz@beuth-hochschule.de

S. Junne
Laboratory of Bioprocess Technology, Institute of Biotechnology, Technische Universität Berlin, Ackerstrasse 71-76, ACK 24, 13355 Berlin, Germany

M. Nicolas Cruz-Bournazou
Department of Process Dynamics and Operation, Institute of Process Engineering, Technische Universität Berlin, Straße des 17. Juni 135, KWT 9, 10623 Berlin, Germany

A. Angersbach
Biotronix GmbH, Neuendorfstrasse 24a, 16761 Hennigsdorf, Germany

Introduction

During bioreactor cultivations, common measurements as the cell dry weight, concentration of substrates and products, or the composition of the exhaust gas are often used for controlling. However, all these data do not provide detailed information on the physiological state of the cell. Recent advances in application of flow cytometry [1, 2], where several parameters can be monitored simultaneously, try to overcome this lack of knowledge. These techniques were applied to follow the time course of viability of cells in batch, fed-batch, and continuous cultures [3–5]. In these experiments, the viability, that is the membrane potential of the cells, permanently changed during cultivation. When cells were sorted in several fractions from viable to non-viable cells, this change was reflected in their classification [3]. Earlier studies already revealed cell membrane potential dynamics in *Escherichia coli* batch fermentations [6]. These changes with a peak in the early exponential phase were found to be concomitant to the DNA replication. It was assumed that the metabolic activity was at a maximum to support energy for the intracellular processes.

Evaluation of forward angle light scatter (FALS) signals showed a continuous change in morphology throughout the exponential growth phase in batch cultivations as well. The steep change during the early exponential phase was independent from the development of the cell size. The cause for this effect is a change in structure and chemical composition of the cytoplasma [7].

In our study, the polarizability was determined in *E. coli* batch cultivations continuously with at-line electrooptical measurements without the utilization of staining methods. Electrooptical measurements measure the change in the orientation of bacteria exposed to an electrical field based on the change in the absorption of orthogonally located light beams. The change in the absorption relative to the state, when no electrical field is applied, reflects the magnitude of the cell polarizability. While the electrical field acts on the cells, a charge is induced on the boundaries of the cell structures. This charge depends on the different dielectric properties of the cell. When the induced charges on the surface of the cells are exposed to an electrical field, a moment of rotation acts on the cells, effecting a change in cell orientation. This reorientation causes an alteration of the absorption characteristics of the cell suspension [8].

For mathematical description of polarizability, a tensor is used, which consists of one longitudinal and two transversal components. This tensor of polarizability $\alpha(\omega)$, which is dependent of the electrical field frequency ω, is a quantitative parameter characterizing the spatial distribution of induced charges and their absolute values. They are a function of the ratio of the complex dielectric permeability ε of neighboring cell structures. The difference of the longitudinal and transversal components leads to the frequency dependent anisotropy of polarizability (FDPA):

$$d\alpha(\omega) = \alpha||(\omega) - \alpha\perp(\omega) \quad (1)$$

with $\alpha||(\omega)$ being the longitudinal component of polarizability and $\alpha\perp(\omega)$ being the transversal component in Eq. (1) [9]. The signals that are obtained when the optical density is measured change due to the reorientation. Since this method takes only a few seconds, a high sample frequency can be applied. Furthermore, when considering the time of relaxation after the electrical field is shut off, the length of the bacterial cells can be determined. After the reorientation of longer cells in the electrical field, it will require more time for relaxation after shutting off the electrical field to return to the original isotropic steady state.

So far, several studies describe dynamics of polarizability depending on changes due to phage interaction and the induction of recombinant protein production in *E. coli* [8, 10]. However, the frequency of measurements was low because manual sample preparation was time-consuming. In our present study, we follow the hypothesis that automated at-line monitoring of electrooptical properties with high temporal resolution can provide valuable information on the metabolic state of cells.

Materials and methods

Bacterial strain and media

The strain *E. coli K12* DSM 498 was used throughout this study. Media components were purchased from Carl Roth (Karlsruhe, Germany) if not otherwise stated. At all batch cultivation experiments, a medium was used containing (per liter) 10 g glucose, 5 g yeast extract (Deutsche Hefewerke, Hamburg, Germany; the same batch used in all experiments), 3 g K_2HPO_4, 1.5 g KH_2PO_4, 1.25 g $(NH_4)_2SO_4$, 0.1 g $MgSO_4 \bullet 7H_2O$, 0.037 g $Na_2EDTA \bullet 7H_2O$, 0.01 g NaCl, and 0.001 g $FeSO_4 \bullet 7H_2O$. Glucose was autoclaved separately. The pH was adjusted to pH 7.0.

Cultivation conditions

One milliliter of a shake-flask culture, which had been incubated for 24 h at 37°C on a longitudinal shaker with an amplitude of 25 mm at 150 rpm, was used for inoculation of the pre-culture. The pre-culture had a liquid volume of 150 ml and was grown at the same conditions for 16 h, otherwise as stated in the results section.

Bioreactor cultivations were performed in stirred tank bioreactors KLF 2000 (Bioengineering AG, Wald, Switzerland) with a cultivation volume of 2 l minimum. The aeration rate was set to 1.0 vvm at an impeller speed of 800 rpm. The cultivation temperature in the batch experiments was set to 28, 32, and 37°C, respectively. The pH (setpoint at 7.0) was kept constant by controlled addition of 30% (w/v) NaOH solution or 10% HNO_3 (w/v) solution. The dissolved oxygen concentration was measured with an Ingold DO-sensor (Mettler-Toledo, Giessen, Germany). Under the applied aeration rate, the dissolved oxygen concentration never decreased below 25% of saturation at all experiments. Oxygen in the off-gas was analyzed with a Maihak Oxygor 6 N and carbon dioxide was measured with a Maihak Unor 6 N (both Sick Maihak, Reute, Germany). Polyethylene glycol 3000 (Sigma-Aldrich, Munich, Germany) was used to reduce foam formation. Two independent bioreactor cultivations were performed for every set of cultivation conditions.

Product analysis

The optical density at 620 nm was monitored every 15 s with a spectrophotometer EloChek (Biotronix, Hennigsdorf, Germany) by circulating culture suspension in a bypass from the reactor through a flow cell with an optical

depth of 2.2 mm. Due to this small distance, the measurement of the optical density was within the linear range of the Lambert–Beer law throughout all bioreactor cultivations. Biomass concentration was additionally determined off-line with appropriately diluted samples at 600 nm in a spectrophotometer PM2 A equipped with a 10-mm flow cell (Carl Zeiss, Oberkochen, Germany).

Glucose concentration in the supernatant was determined using the enzymatic glucose liquiUV^{mono} test (Human Diagnostics, Wiesbaden, Germany) in a Beckman DU 640 UV–VIS spectrophotometer (Beckman Coulter, Fullerton, CA) at 340 nm following the supplier's instructions. Acetate concentration was determined at the same wavelength applying the enzymatic acetate test kit from Boehringer Mannheim/R-Biopharm (Mannheim, Germany) according to the manufacturer's instructions. Prior to enzymatic determination, cells were separated from the supernatant with centrifugation at 10,000 rpm for 15 min.

Determination of polarizability anisotropy (AP) and mean cell length

The fully automated measurement system EloTrace (Biotronix, Hennigsdorf, Germany) was used to monitor the polarizability anisotropy (AP) and mean cell length of *E. coli* in a sampling interval of 10 min. Cells were separated from the culture broth by filtering through a cellulose filter (pore size 0.45 µm, Sartorius, Goettingen, Germany). The cell concentrate was diluted with distilled water of a conductivity of 5 µS/cm to a final optical density of $A_{600} = 0.1 \pm 5\%$ prior to the electrooptical measurement. The AP was acquired in a measurement chamber at four frequencies: 210, 400, 900, and 2,100 kHz, respectively, after the changes of optical density due to reorientation reached a steady state [9]. The unit of experimental values of AP includes a scale coefficient, therefore being 5×10^{-31} Fm^2.

The mean cell length was determined based on the relaxation characteristics of the cell suspension after the electrical field is shut off. The system was calibrated in advance by measuring the length of a representative amount of cells on microscopic photographs and correlating these results to the measured relaxation time.

Data analysis

Curve fits for evaluation of rates from concentration time series data were derived with the curve-fitting toolbox in MATLAB version 7.0.1 (MathWorks, Natick, MA) using polynomial or smoothing spline approximation. For principal component analysis (PCA) [12], data were normalized prior to calculation. For developing and testing the model, a partial-least squares (PLS) method or multilinear PLS (N-PLS) was applied [13]. PLS model derivations were performed with the PLS Toolbox version 4.2 for MATLAB (Eigenvector Research, Manson, WA), N-PLS models were generated with m-files from the N-way toolbox [14]. The SIMPLS algorithm was used for factor determination [15]. The data of AP measurement and specific acetate uptake rates were mean-centered. The number of factors for the model were chosen on the basis of the root mean square error of calibration (RMSEC):

$$\mathrm{RMSEC} = \sqrt{\frac{\sum_{i=1}^{n} (\overline{y}_i - y_i)^2}{n}} \quad (2)$$

where y_i are the calibration values, $\overline{y}_i$ the values predicted by the model and n the number of calibration samples. The root mean square error of prediction (RMSEP) was calculated following Eq. (2), except that y_i were not the calibration but test values.

Results

Effects of temperature variation on the polarizability anisotropy in batch cultivations

In Fig. 1, for a cultivation at 32°C the AP determined at 210 kHz and the mean cell length are shown together with further state variables, rates, and parameters. The time pattern of the AP in the two independent experiments is reproducible. It can be compared to the time course of the cell membrane potential measured in *E. coli* batch fermentations with the help of fluorescent staining and flow cytometry [6]. An increase of AP can be observed during the first 2 h of cultivation, the lag-phase, and the early exponential phase. Here the specific glucose consumption (qGlucose) reaches maximum values while a strong increase in specific acetate synthesis (qAcetate) can be observed. During the next 3 h, AP drops off and the glucose concentration is reduced to 5 g/l (no substrate limitation) at $t = 5$ h. During this phase, the highest biomass growth and specific oxygen uptake (qO_2) and carbon dioxide consumption (qCO_2) rates are measured. Also, the highest biomass yield is achieved.

In the following 4 h of cultivation until $t = 9$ h, the culture is still growing and glucose is not limiting. However, the specific growth is declining and the decline of AP changes its slope to a slow decrease. When the culture enters the stationary growth phase as glucose is depleted and biomass increase stops at $t = 9$ h, the beginning of acetate uptake is characterized by a slight increase of polarizability (cf. also Fig. 3).

In Fig. 1, the mean cell length is shown for two independent experiments. The dynamics of mean cell length

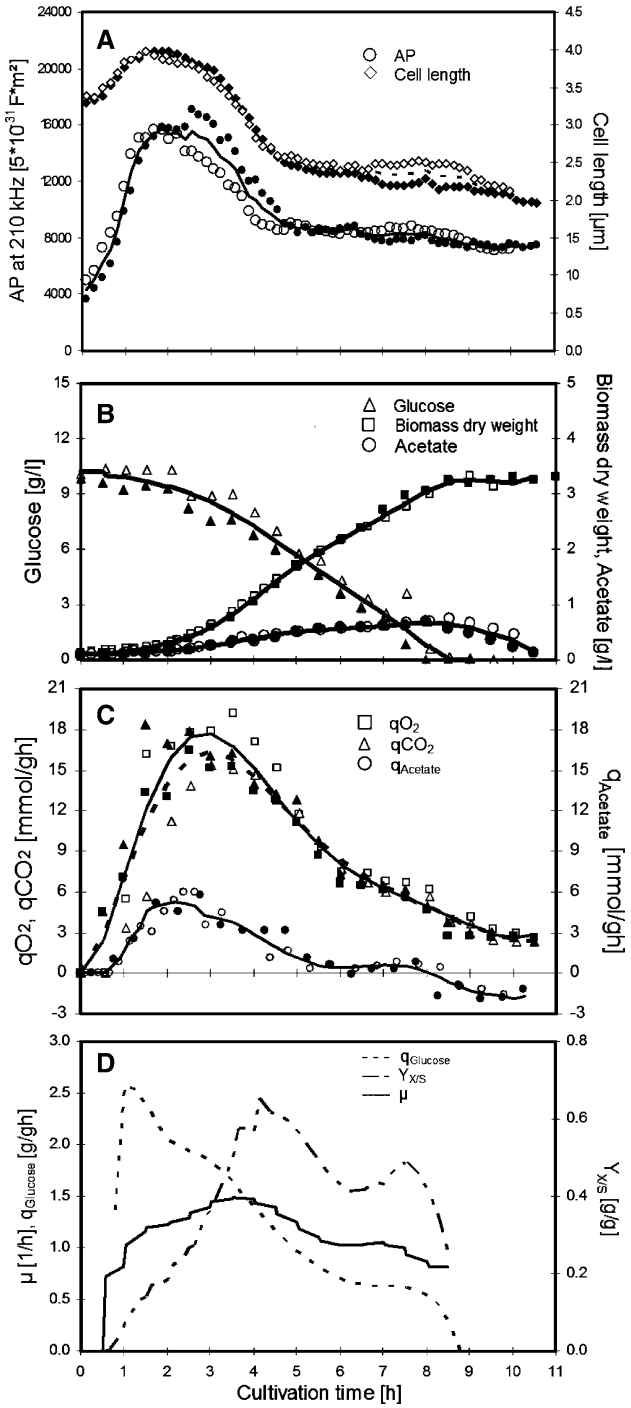

Fig. 1 Summary of cultivation parameters and variables in *E. coli* batch cultivations at 32°C. *Open* and *closed signs* represent the same parameters of each independent experiment. *Lines* represent curve fits

determined with electrooptical measurements are more pronounced in the lag and growth phase than at the time when growth retards. After the mean cell length increases during the first 2 h of cultivation, a continuous decrease from 4.0 to 2.0 µm is observed. Dynamic behavior of AP and mean cell length is similar in this case.

In Fig. 2, the dependence of polarizability on frequency between 90 and 160 min after inoculation is most pronounced. This is also the phase of the strongest acetate synthesis activity. Before and after this phase, the dependence of polarizability on the frequency in the observed range in between 210 and 2,100 kHz is rather low.

For comparing the effects of changed metabolic activity on the cell polarizability when cultivating at different temperatures, experiments were repeated at 37 and 28°C. In batch cultivations at 37°C, a higher cell polarizability is detected soon after inoculation (Fig. 3). The polarizability rises sharply during the first 1.5 h. In the following, a sharp decline is observable, which changes its slope to a slow decline after 3 h of cultivation. In experiments at 28°C, a similar behavior during the first hours of cultivation is observed. In comparison to the experiments at 37 and 32°C, the decline of polarizability is delayed further. The mean of the average polarizability for the first 10 h of cultivation decreases from the experiments at 28°C to those at 37°C (Table 1). The higher the temperature-dependent metabolic activity, that is specific glucose consumption, growth, and acetate synthesis as well as specific carbon dioxide production, the faster the polarizability reaches its maximum and declines thereafter. In accordance, the mean average polarizability develops similar to the mean biomass yield and opposite to the acetate concentration at experiments with 16 h of incubation, since the biomass yield is lower when more acetate is produced.

The different temperatures cause a similar time delay in the development of the mean cell length (Fig. 4). The reduction of the mean cell length starts when the culture is in the exponential growth phase and when the maximum of the specific glucose consumption had passed. Hence, the mean cell length is larger in experiments at 28°C than at 32 and 37°C during the first 10 h of cultivation.

Effects of pre-cultivation variation on the polarizability in batch cultivations

When the pre-culture is grown overnight, the cells for inoculation are in the stationary phase. In order to observe whether polarizability and mean cell length during the batch cultivation are affected when the inoculum is physiologically different, the pre-culture was grown for only 2 h. After this time, the pre-culture is in the exponential growth phase. All other conditions were identical to the previously discussed experiment ($T = 37$°C).

As can be seen in Fig. 5a, the polarizability differs during the first 5 h, when the polarizability is comparably low. An initial polarizability of 1×10^{-27} Fm^2 is measured, which is the lowest value among all cultivations. Peak values are reached only after 4 h. Opposite to the

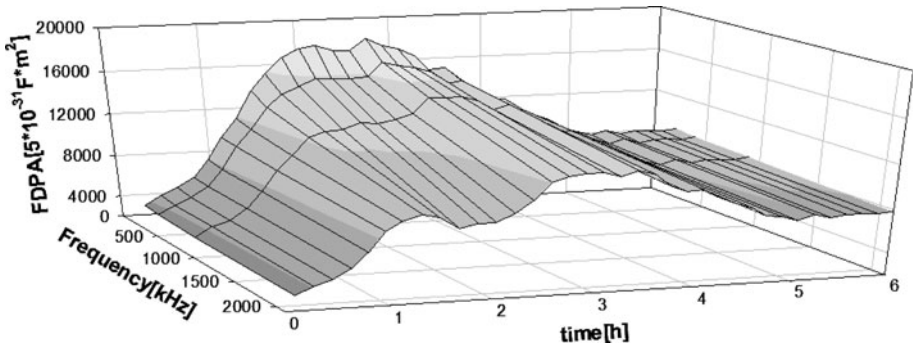

Fig. 2 Development of the FDPA in *E.coli* batch cultivations at 32°C in the first 6 h after inoculation

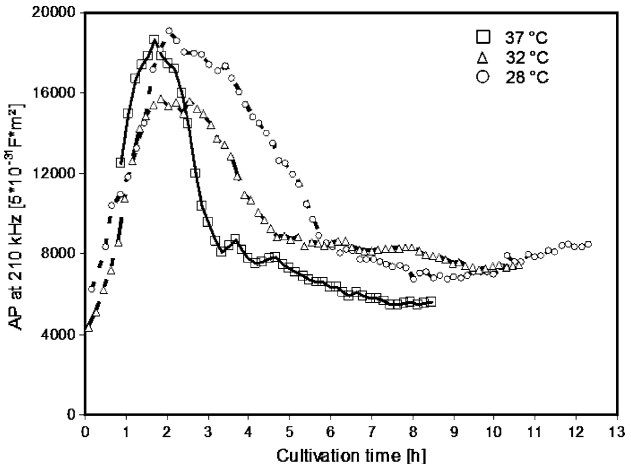

Fig. 3 Development of the average polarizability anisotropy at different temperatures in *E.coli* batch cultivation inoculated with an overnight grown pre-culture

other cultivations, the dynamics of mean cell length are not similar to dynamics of the polarizability.

The initial mean cell length of 4.7 μm is very high due to the cells being in the exponential growth phase. The mean cell length decreases throughout the whole cultivation (Fig. 5b), its time average being similar to that in the cultivations at 28°C (Table 1). Comparing results for the 2-h incubated pre-culture with the three other experiments which exhibit a systematic development, neither data in Table 1 nor the dynamic behavior do fit well into the system. However, there is a strong correlation between the dynamics of the specific acetate synthesis rate (Fig. 6) and the polarizability in all experiments.

Correlation between specific acid synthesis rate and polarizability

A calibration model is developed for testing the hypothesis of a correlation between specific acid synthesis rate and FDPA. A good prediction is possible when the FDPA and its first derivative with respect to the time are used as prediction parameters. With the help of a PLS algorithm, a model is calibrated including the FDPA at the four frequencies at which the polarizability was measured (210–2,100 kHz). The model is created applying a multi-way partial least-squares method (N-PLS).

The root mean square error (RMSEC and RMSEP, respectively) does not exceed 0.28 with this method. The RMSEC and RMSEP among all batch experiments is 0.19. The quality of calibration/prediction is similar at all phases of cultivation (Fig. 7). Hence, the calibration model based on one of the performed experiments is suitable to predict the acetate synthesis rates at all other experiments without any further calibration. A correlation between the physiological parameter cell polarizability and the specific acetate synthesis rate is obvious. These results further support the observations that a division in four fermentation stages during growth is possible by means of electrooptical measurements: (1) a first phase of increasing polarizability, where the bacteria adapt to the conditions in the bioreactor after incubation and where maximum specific glucose consumption rates are reached; (2) a second phase where the polarizability is strongly decreasing, and when the maximum biomass yield is achieved while the culture is growing exponentially; (3) a phase when the polarizability is slowly decreasing or constant, while growth starts to retard; and (4) a phase when polarizability recovers slightly when acetate is taken up by the microorganism while other substrate sources are depleted.

Discussion

This is the first study in which the FDPA and mean cell length were observed at-line with a fully automated sampling procedure, enabling a high measurement frequency. The observed time course of the average polarizability of the cells as well as the mean cell length develop differently at the temperatures and pre-cultivation conditions applied. A correlation between the polarizability and the rate of specific acetate synthesis is observed. Similar results were obtained in a previous study, where it was reported that the fluxes of acids correlate with the FDPA during cultivation of *Clostridium acetobutylicum* fermentations [11].

Table 1 Overview of results from batch cultivation experiments under varying conditions. The absolute deviation between each of the two independent experiments is denoted in *brackets*

	Units	37°C, 16 h of pre-culture incubation Maximum/time average (deviation)	32°C, 16 h of pre-culture incubation Maximum/time average (deviation)	28°C, 16 h of pre-culture incubation Maximum/time average (deviation)	37°C, 2 h of pre-culture incubation Maximum/time average (deviation)
Polarizability—210 kHz	5×10^{-31} Fm^2	18,622/9,245 (±731)	15,729/10,671 (±213)	19,097/12,120 (±31)	14,759/9,672 (±272)
Mean cell length	µm	3.93/2.39 (±0.10)	3.92/2.90 (±0.09)	3.92/2.97 (±0.02)	4.66/2.99 (±0.12)
Biomass concentration	g/l	3.13/1.82 (±0.05)	3.21/1.51 (±0.12)	2.04/0.91 (±0.01)	2.56/1.06 (±0.14)
Maximum growth rate	1/h	1.13/–(±0.02)	0.69/–(±0.08)	0.51/–(±0.01)	1.31/–(±0.09)
Spec. glucose consumption	g/gh	3.95/1.24 (±0.27)	2.57/1.18 (±0.17)	2.59/0.99 (±0.11)	3.15/2.10 (±0.50)
Acetate concentration	mMol/l	21.88/14.18 (±0.49)	14.65/8.5 (±0.31)	7.61/5.07 (±0.01)	17.31/8.54 (±0.62)
Spec. acetate synthesis rate	mMol/gh	12.24/3.11 (±0.12)	5.86/2.53 (±0.09)	3.86/1.98 (±0.01)	9.93/3.42 (±0.08)
Biomass yield	g/g	0.33/0.27 (±0.015)	0.40/0.31 (±0.042)	1.00/0.49 (±0.08)	0.35/0.24 (±0.01)
Specific O_2 uptake rate	mMol/gh	38.55/18.47 (±0.87)	17.70/10.94 (±0.83)	3.36/1.44 (±0.02)	27.46/17.34 (±1.71)
Specific CO_2 production rate	mMol/gh	27.78/13.62 (±0.98)	16.25/10.45 (±1.00)	3.34/1.20 (±0.03)	27.26/15.79 (±1.15)

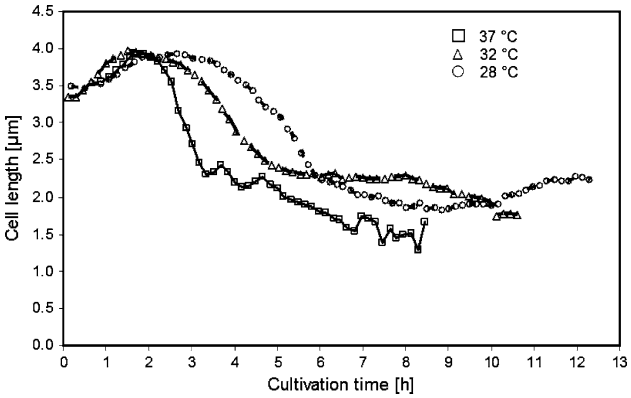

Fig. 4 Development of the average cell length at different temperatures in *E.coli* batch cultivation inoculated with an overnight-grown pre-culture

There might be several reasons for all these observations. The energy metabolism in *E. coli,* which influences substrate uptake and therefore also the synthesis of acetate, may be one of the main influencing factors causing the development of the polarizability. In *E. coli*, acetate synthesis and excretion occurs during the so-called 'overflow metabolism' [16] at excess substrate. Acetate accumulation is observed at high glucose consumption rates and high specific growth rates [17]. The carbon flow through pyruvate (and to some extent acetyl-CoA) is partly shifted towards acetate production instead of entering into the tricarboxylic acid cycle [18, 19].

It can be assumed that the amount of acetate produced has—directly or indirectly—a negative influence on the polarizability. When peak levels of polarizability are reached, the acetate synthesis is high and the polarizability starts to decrease faster than at low rates of acetate synthesis. The measured polarizability is evoked mainly by the Maxwell–Wagner polarization mechanism. It relies on the accumulation of electric charges at the interface of two media of different electrophysical properties. In the case of bacteria, these are the cytoplasm and its membrane. While the acetate concentration rises, dissociated acetate accumulates inside the cell [20]. The intracellular ion balance changes [21], influencing the Maxwell–Wagner polarizability. Measurements of the intracellular ratio of NADH and NAD^+ (data not shown) revealed significant changes in parallel to the development of the polarizability. It can be assumed that the energy balance of the cell, which influences acetate synthesis [22], also has an effect on this parameter.

The correlation is also valid at a reduced pre-cultivation time, although the time pattern of polarizability and mean cell length is shifted. The environment to which the cells are exposed in the different pre-cultures leads to different resistance mechanisms, e.g., an altered membrane

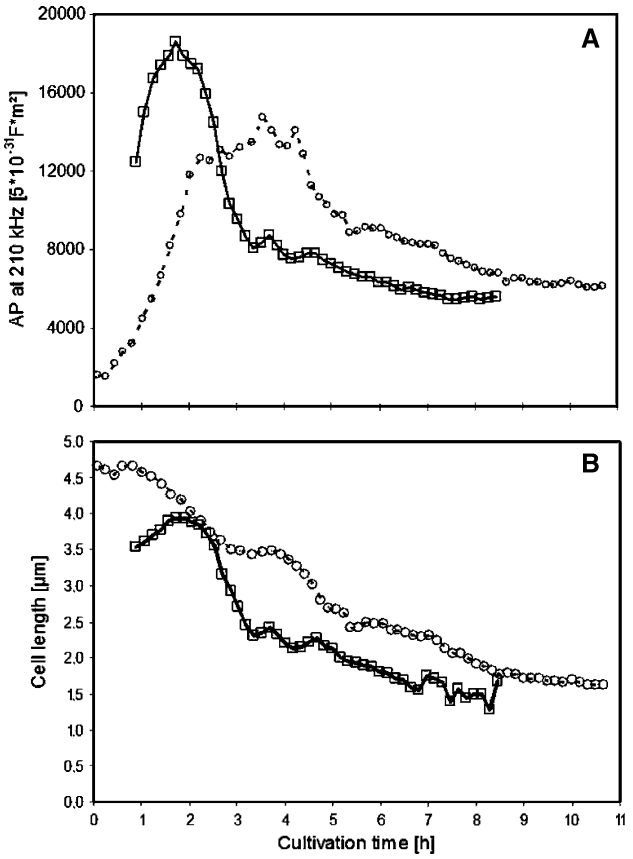

Fig. 5 Development of the average polarizability anisotropy (**a**) and average cell length (**b**) in *E. coli* batch cultivation operated with an overnight-grown preculture (*open square*) and 2 h of pre-cultivation (*open circle*)

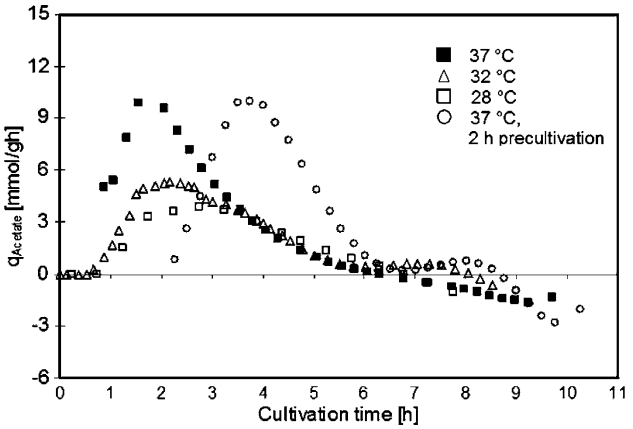

Fig. 6 Development of the specific acetate synthesis rates in *E.coli* batch cultivation operated at different temperatures and pre-cultivation conditions

composition [23, 24]. In our case, the polarizability is an indicator for the time that is needed for the microorganism to recover from the lag phase. The higher the polarizability, the shorter is the lag phase.

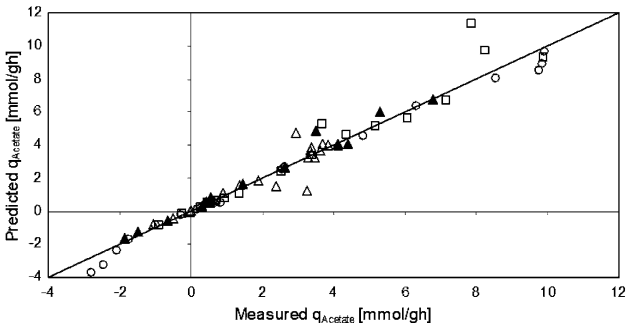

Fig. 7 Accuracy of model prediction of the specific acetate synthesis rate in batch cultivations operated at 37°C (*open diamonds*) and at 28°C (*open triangles*) (each inoculated with an overnight-grown pre-culture), as well as at 37°C inoculated with a 2-h-grown pre-culture (*filled triangle*). For model calibration (*filled square*), the data set of batch cultivations at 32°C inoculated with an overnight grown pre-culture was used

The high values of the mean cell length observed during the onset of batch cultivations agree with the observation that *E. coli* cells are longer at exponential growth than at linear growth [25]. The transmembrane pH gradient and intracellular accumulation of sugar and products such as acid anions can cause a swelling of cells while osmotic pressure increases [21]. If the acetate concentration increases further, the cell wall starts to get permeabilized [26], the osmotic pressure inside the cell is reduced and the observed reduction of size at high acetate concentrations follows. This effect is amplified by starvation at the end of batch cultivations when, because of the lack of educts, membrane repair ceases.

Morphologic parameters, metabolite concentrations, and turnover rates are useful in assessing the quality of a pre-culture and in monitoring the following process during the lag phase. Direct measurement of metabolic activity based on concentrations is difficult at this early time due to low cell densities, and, as a result, low turnover rates. Early information about limitations, especially when compounds of the media can not be easily quantified, is possible by the presented application of electrooptical measurements. The significant dynamics and the high information content of these measurements during the cultivation makes the application of electrooptical methods a valuable tool for process observation.

Our current work on calibration model validation under different cultivation modes shows promising results and will be published in a forthcoming publication. Extension of the method to other microbial systems, especially when exhibiting overflow metabolism, will be a topic of our future research in this area.

Acknowledgments We wish to express our thanks to Peter Neubauer for fruitful discussions.

References

1. Hewitt CJ, Nebe-Von-Caron G (2004) The application of multi-parameter flow cytometry to monitor individual microbial cell physiological state [Review]. Adv Biochem Engin/Biotechnol 89:197–223
2. Shapiro HM (2000) Microbial analysis at the single-cell level: tasks and techniques. J Microbiol Meth 42:3–16
3. Hewitt CJ, Nebe-Von-Caron G, Nienow AW, McFarlane CM (1999) The use of multi-parameter flow cytometry to compare the physiological response of *Escherichia coli* W3110 to glucose limitation during batch, fed-batch and continuous culture cultivations. J Biotechnol 75(2–3):251–264
4. Hewitt CJ, Nebe-Von-Caron G, Nienow AW, McFarlane CM (1999) Use of multi-staining flow cytometry to characterise the physiological state of *Escherichia coli* W3110 in high cell density fed-batch cultures. Biotech Bioeng 63(6):705–711
5. Want A, Thomas ORT, Kara B, Liddell J, Hewitt CJ (2009) Studies related to antibody fragment (Fab) production in *Escherichia coli* W3110 fed-batch fermentation processes using multiparameter flow cytometry. Cytometry 75A:148–154
6. Monfort P, Baleux B (1996) Cell cycle characteristics and changes in membrane potential during growth of *Escherichia coli* as determined by a cyanine fluorescent dye and flow cytometry. J Microbiol Meth 25:79–86
7. López-Amorós R, Comas J, Carulla C, Vives-Rego J (1994) Variations in flow cytometric forward scatter signals and cell size in batch cultures of *Escherichia coli*. FEMS Microbiol Lett 117:225–230
8. Angersbach A, Bunin VD, Ignatov OV (2006) Electro-optical analysis of bacterial cells. In: Stoilov S (ed) Molecular and colloidal electrooptics. M. Dekker Publications, New York, pp 86–112
9. Bunin VD (2002) Electrooptical analysis of a suspension of cells and its structures. In: Somasundaran P, Hubbardt A (eds) Encyclopedia of surface and colloid science. M. Dekker Publications, New York, pp 2032–2043
10. Bunin VD, Voloshin AG, Bunina ZF, Shmelev AV (1996) Electrophysical monitoring of culture process of recombinant *Escherichia coli* strains. Biotech Bioeng 51:720–724
11. Junne S, Klein E, Angersbach A, Götz P (2008) Electrooptical measurements for monitoring metabolite fluxes in acetone-butanol-ethanol fermentations. Biotech Bioeng 99(4):862–869
12. Wold S (1987) Principal component analysis. Chemom Intell Lab Sys 2:37–52
13. Wold S, Geladi P, Esbensen K, Öhman J (1987) Multi-way principal components- and PLS-analysis. J Chemometr 1:41–56
14. Andersson CA, Bro R (2000) The N-way toolbox for MATLAB. Chemom Intell Lab Syst 52:1–4
15. de Jong S (1993) SIMPLS: an alternative approach to partial least squares regression. Chemom Intell Lab Syst 18:251–263
16. Wolfe A (2005) The acetate switch [Review]. Microbiol Mol Biol Rev 69(1):12–50
17. Kayser A, Weber J, Hecht V, Rinas U (2005) Metabolic flux analysis of *Escherichia coli* in glucose-limited continuous culture I. Growth-rate-dependent metabolic efficiency at steady state. Microbiology 151:693–706
18. Phue J-N, Shiloach J (2005) Impact of dissolved oxygen concentration on acetate accumulation and physiology of *E. coli* BL21, evaluating transcription levels of key genes at different dissolved oxygen conditions. Metab Eng 7:353–363
19. Abdel-Hamid A, Attwood MM, Guest JR (2001) Pyruvate oxidase contributes to the aerobic growth efficiency of *Escherichia coli*. Microbiology 147:1483–1498
20. Diez-Gonzalez F, Russell JB (1997) The ability of *Escherichia coli* O157:H7 to decrease its intracellular pH and resist the toxicity of acetic acid. Microbiology 143:1175–1180
21. Roe AJ, McLaggan D, Davidson I, O'Byrne C, Booth IR (1998) Perturbation of anion balance during inhibition of growth of *Escherichia coli* by weak acids. J Bacteriol 180(4):767–772
22. Vemuri GN, Altman E, Sangurdekar DP, Khodursky AB, Eiteman MA (2006) Overflow metabolism in *Escherichia coli* during steady-state growth: transcriptional regulation and effect of the redox ratio. Appl Environ Microbiol 72(5):3653–3661
23. Yuk H-G, Marshall DM (2004) Adaptation of *Escherichia coli* O157:H7 to pH alters membrane lipid composition, verotoxin secretion, and resistance to simulated gastric fluid acid. Appl Environ Microbiol 70(6):3500–3505
24. Kannan G, Wilks JC, Fitzgerald DM, Jones BD, BonDurant SS, Slonczewski JL (2008) Rapid acid treatment of *Escherichia coli*: transcriptomic response and recovery. BMC Microbiol 8(37). http://www.biomedcentral.com/1471-2180/8/37
25. van de Merwe WP, Czégé J, Milham ME, Bronk BV (2004) Rapid optically based measurements of diameter and length for spherical or rod-shaped bacteria in vivo. Appl Opt 43(28):5296–5302
26. Russell JB, Diez-Gonzalez F (1998) The effects of fermentation acids on bacterial growth. Adv Microb Physiol 39:205–234